Near-field Beam and Cross-polarization Pattern Measurement of ALMA Band 8 Cartridges

Masato Naruse[1,2,*], Mamoru Kamikura[1,2], Yutaro Sekimoto[1,2], Tetsuya Ito[2], Masahiro Sugimoto[2], Yoshizo Iizuka[2],

[1]*Department of Astronomy, University of Tokyo, Japan*
[2]*National astronomical Observatory of Japan*
* Contact: masato.narsue@nao.ac.jp, phone +81-422-34-3981

Abstract—We meas ured corrugated h orns, O MTs [1] (Orthomode T ransducer), op tics b locks at room temp erature with a vecto r near fi eld m easurement s ystem. Th e amp litude and phase me asured at ne ar-field a re transformed to far-field pattern, and compared to calculations with Gr asp 9 and CORRUG . The c o-polar beams were found to be c onsistent with the simulations at 385 , 442, 500 GHz, and the calcula ted taper efficiency at the sub-reflector of ALMA 12-m antenna was greater than 92 % . Side lobe was less than -30 dB. The peak of cross-polar relative to co-polar found to be less than -20.5 dB. In addition, to evaluate accuracy of m easurements, we stu died both effects of standing w ave and stability of t he amplitude and phase. The error of the far-field was found to be less than 0.2dB between 0 and -20 dB range.

I. INTRODUCTION

The Atacama Large Millimeter/submillimeter Array (ALMA) [2] is an interferometer for radio astronomical observations. The development of this facility is the result of an international effort between Europe, North America, and Japan in cooperation with the Republic of Chile. ALMA consisting of 64 12-meter diameter antennas and 16 ACA (Atacama Compact Array) antennas is located in Chile at an elevation of 5000 meters. At this elevation the atmosphere has a maximum transparency at mm and sub-mm wavelength. ALMA will cover the radio sepctrum from 30 to 950 GHz using 10 frequency distinctive bands with relatively wide bandwidth of around 25 %. Each frequency band is observed with a cartridge-type receiver with orthogonal polarization-receiving capabilities. The cartridge-type receiver contains optics, mixers, amplifiers and local oscillators to achieve a modular concept. The cartridges are installed in a cryostat at the Cassegrain focus with an offset for the telescope axis. Each cartridge has receiver optics in itself or outside of the cryostat toward the sub-reflector. The receiver optics of ALMA has been described by [3]. It does not use a mechanical tuner in the receiver because of operational reliability.

A physical optics calculation of the ALMA receiver optics was made by [4], [5]. It uses a commercial software, GRASP9 (TICRA Co.).We have repeated their calculation with the same software. The beam pattern of corrugated horns is simulated with a commercial software, CORRUG (Antenna Software Co.).

For astronomical receivers, it is essential to understand the beam pattern on the sky. Since ALMA receivers are installed on the Cassegrain focus of the antenna, the beam pattern of the receiver directly determines that of the telescope. Since ALMA makes polarization observations of astronomical sources, it is also critical to know its cross-polarization pattern. On the symmetrical Cassegrain system, cross-polarization components are mainly generated at the receiver. It is important to measure beam pattern at the same or a similar condition of operational 4 K temperature for SIS receivers. In addition, room temperature measurements are useful for a selection of corrugated horns. Because corrugated horns are fabricated by electroforming, it is not possible to know their performance using easy mechanical measurements.

We designed and developed a near-field measurements system according to the experience maturated in the field of beam pattern measurements at sub-mm wavelength in the past 20 years. A near-field measurement, and probe compensation concept have been established ([6], [7], [8]), ([9], [10]), respectively. Sub-mm beam pattern measurements were reported in [11], [12], [13] and vector measurements in [14], [15]. Other examples of room temperature measurements of sub-mm receiver optics and corrugated horns are documented in [16], [17]. We established the beam pattern measurements of both receiver components at room temperature and the receiver itself as both detector and antenna under test (AUT). Owing to its wide dynamic range, the cross-polarization pattern of the receiver is also reported.

II. ALMA BNAD 8 CARTRIRGE

The ALMA band 8 cartridge receives [18] frequency from 385 GHz to 500 GHz, which is 26 % bandwidth to the center frequency of 442.5 GHz. We have developed a pre-production model (PPM) of the ALMA band 8 cartridge. The ALMA band 8 PPM receiver [19] is a dual polarization receiver, which uses a OMT as a polarization splitter. The receiver optics block adopts a single mirror to couple the feed horn in front of the mixer and the sub-reflector. One of the advantage of adopting a single mirror system is the relative easiness at the optical alignment. It leaves, however, less freedom for the mechanical designs. The incident angle at the mirrors is as small as 25 ° (Figure 1), which aim is to keep

the cross-polarization as low as possible [20]. The optical parameters were chosen as frequency independent at both the feed horn and the sub-reflector in the frequencies of between 385 and 500 GHz as listed in Table 1. The proof of this is shown in Figure 2, where the symmetric and asymmetric electric field distribution cuts are reported for the lowest, middle and highest frequencies. The receiver optics is tilted 1.2 degrees toward the sub-reflector.

The optics block was carefully designed to realize the optical parameters at 4 K [21]. The shrinkage of all components from 300 K to 4 K was taken into consideration. The block was designed to be easily measured with a coordinate machine. Optical block and mirrors were made of pure aluminum. The optics block and mirrors were measured mechanically with a coordinate measuring machine, resulting in consistency with designed values within typically 20 μm.

The corrugated horn, which design is reported in [22,23], has a diameter of 8 mm and a slant length of 24.43 mm. Due to the fine structure of the corrugations, the horn and the transformer waveguide, which connects the horn to the rectangular waveguide, were made in one piece using electroforming machining technique.
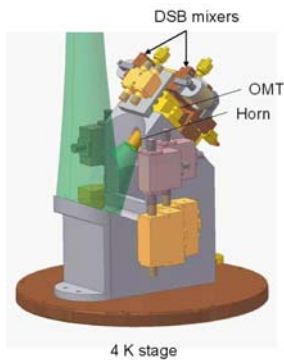

Fig. 1 The 4K Optics of Band8 Cartridge Receiver

TABLE I
OPTICAL PARAMETER OF ALMA BAND 8 CARTCIDGE

|		Band 8	385	442	500
horn diameter	d_h	7.99			
horn axial length	L_h	24.10			
horn slant length	R_h	24.43			
horn waist	w_0		1.736	1.603	1.482
horn waist offset	$dz_{(w_0)}$		-13.291	-14.933	-16.319
waist at horn aperture	w_{ha}		2.572	2.572	2.572
distance from mirror to horn	d_1	50			
radius of curvature	R_{s1}		66.133	67.529	68.637
focal length of mirror	f_1	49.59			
radius of curvature	R_{il}		198.227	186.663	178.690
beam radius at mirror			9.200	8.890	8.671
reflection angle of mirror	θ_1	45			
waist at focal plane	w_{fp}		4.7018	4.0955	3.6205
distance from mirror to subref	$d_{mirror-subref}$	6150			
beam radius at subref	w_{subref}		316.27	316.27	316.27
radius of subref	R_{subref}	375			
Edge taper		12	12.21	12.21	12.21
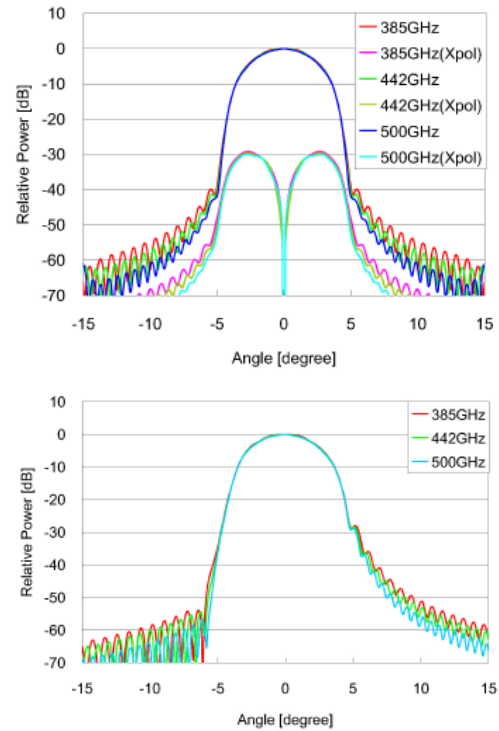
Fig. 2 Physical Optics calculation of the 4K optics with Grasp9. Upper and lower panels show beam pattern of a symmetric and asymmetric plane.

III. INSTRUMENT

A. Submillimeter Vector Network Analyzer

In order to measure amplitude and phase of electromagnetic field distribution, a submillimeter network analyzer, (Figure 3) a $XYZ\theta$ planar scanner, and probe horns have been developed [24]. The band 8 RF signal is obtained with a Gunn oscillator source tuned at 77-110 GHz, followed by a x5 multiplier. The transmitter chain is located on the $XYZ\theta$ planar scanner as shown in figure 3, while the receiver which has the optics under test connected at the harmonic mixer is located on a test bench. The whole system uses a common reference signal at the frequency of 10 MHz. This reference signal is used to phase lock the Gunn diode and as reference for the generation of the LO signal. The LO signal is used to generate the higher harmonics of the Gunn oscillator signal through a harmonic mixer. The LO signal frequency is chosen such as the 6th harmonic equals the 10 MHz reference signal for phase locking. On the receiver side the LO signal is mixed with the RF signal in order to obtain the 30th harmonic which is giving the 50 MHz signal. Amplitude and phase information of the RF signal are then measured by the vector voltmeter which compares the 30th harmonic with the reference signal multiplied.
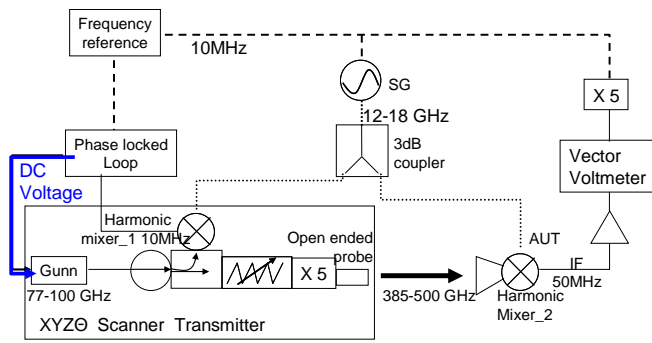
Fig. 3 Block diagram of near-field beam measurement system of receiver components with a room-temperature mixer. PLL controls the frequency of Gunn varying the DC Voltage.

Fig. 4 A picture of beam pattern measurement system configuration

B. Planar XYZθ Scanner

A planar XYZθ scanner for submillimeter-wave measurement is highly necessary for flatness [25, 26]. A XYZθ scanner has been employed to accommodate a cartridge test cryostat (Figure 5), which was developed for testing cartridge type receivers [27]. The XYZθ scan area is 300 mm × 300 mm × 600 mm and -180 degrees to 180 degrees, which is driven with 10 μm and 0.1 degree step by stepping motors. The motors are controlled via GPIB interface by LabView software. The Z stage of this scanner was used to investigate VSWR of the measurement configuration. The absorber was appropriately installed to reduce VSWR. The θ stage of this scanner was used to measure the cross-polarization pattern and the alignment of the polarization. The flatness of this scanner has been measured as follows:

1. A flat aluminum mirror with a diameter of 300 mm was fabricated for reference with a high precision lathe (Toshiba Co. ULG-300C H3).

2. The reference mirror was measured with 0.1 μm accuracy by a coordinated machine (Mitsutoyo LEGEX910). The flatness of the reference mirror was 2 μm peak to peak.

3. The flatness of the XYZθ scanner relative to the reference mirror was measured with a laser sensor of Kyence LK-500, which has a resolution of 10 μm at 690 nm wavelength. After removing the linear component, the flatness was 4.3 μm r.m.s. and 17.2 μm peak-to-peak for horizontal axis and 3.3 μm r.m.s. and 13.5 μm peak-to-peak for vertical axis.
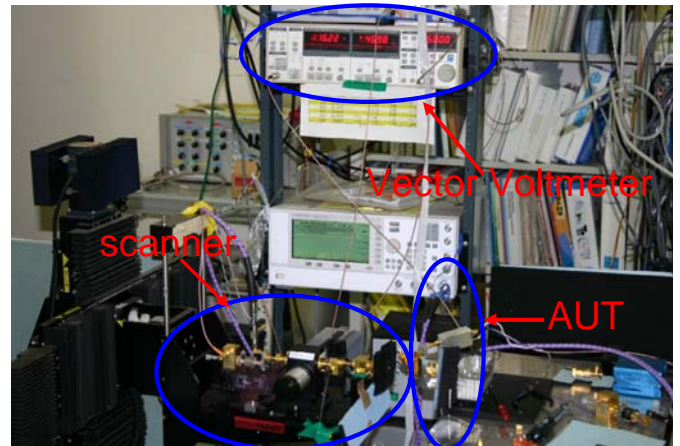
C. System Stability and Standing Wave Characterization

Reproducibility and accuracy of the beam pattern measurements is directly related by intrinsic system stability over the time of measurement. The issue of standing wave phenomena is also affecting the quality of the beam pattern structure. Amplitude and phase stability over a time of one hour is shown in Figure 5. It can be seen that 0.2 dB amplitude and 2 degree phase stability are obtained in 5 minutes span. Since a typical 2D scan takes 4 hours, the long term amplitude and phase drift are corrected by periodically referencing at the main beam peak at every 5 minutes.

In Figure 6 the effect of standing wave in relation to the measurement plane is reported. The plot shows the superposition of 9 far-field cuts of consecutive near-field line scans taken at a distance of λ/4 from each other. TK-RAM (Thomas-Keating Co.) was installed at the transmitter and receiver sides. The effects of the standing wave at 385, 442 and 500 GHz were measured at the same level and to be at typical minimum level of 0.5 dB peak-to-peak. The effects of the standing wave at 385, 442 and 500 GHz were at the same level. The measurement repeatability was evaluated by measuring the band 8 corrugated horn 9 times at the same location. The difference between these measurements gave a 0.1 dB and 1 dB amplitude variation respectively at the level of -25 and -40 dB.

The return loss of submillimeter components such as a corrugated horn was derived from standing wave ratio (SWR). For example, the lower panel of Figure 6 shows the SWR of a corrugated horn radial offsets from beam center. These SWR are averaged to convert the return loss. At large offsets, the SWR has a tendency to increase. It may be caused by reflection from metal components of measurement support structure.
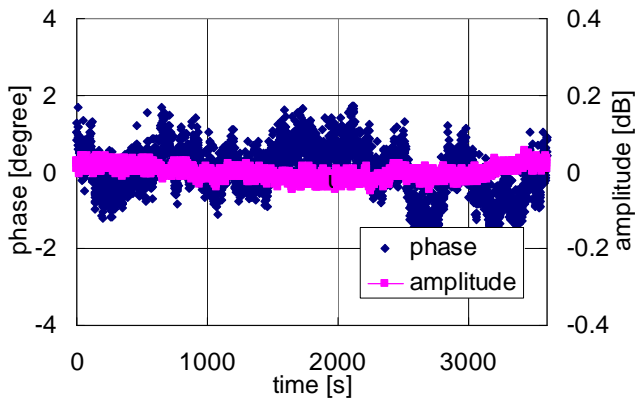
Fig. 5 Amplitude and phase stabilities of this system at room temperature, and RF frequency of 442 GHz and IF frequency of 50 MHz.
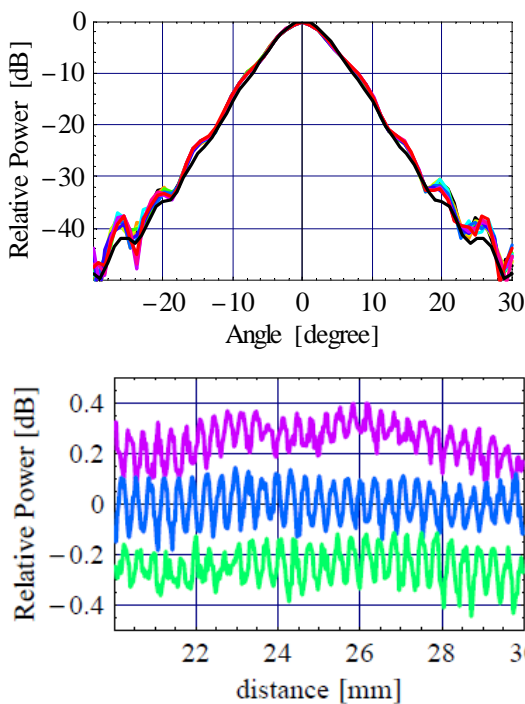

Fig. 6 Upper:Standing measurement at 442 GHz with the corrugated horn. The 9 lines with every 1/4 λ moving and simulation with CORRUG (black line) are superimposed. Lower:The standing wave of a corrugaterd horn at center and offset position of X-direction at 442GHz. The purple, blue, and green lines respectively show at -4, 0, 4 mm offsets.Power scale of each lines has been offset by 0.25 dB. Rreturn loss of the corrugated horn was derived around -40 dB using the average of three SWR.

D. Submillimeter Probe Horn

When measuring beam pattern with a planar near-field measurement system, it is very important to understand the effects of the probe with on the measured electric field distribution. In [28] it is reported that open-ended waveguides introduce less effects on the measured electric field distribution. Nevertheless we performed probe compensation of the measured near-field beam patterns, by dividing the far-field distribution of the measured field by the far-field distribution of the measured open-ended waveguide probe, [10]. Characterization of the open-ended WR2.0

waveguide was performed by independent measurements of two out of three " identical " probes. Figure 7 shows the electroformed open-ended waveguide surrounded by electromagnetic absorber tiles such as TK-RAM (Thomas-Keating Co.). The improvement achieved in reduction of standing waves is depicted in figure 9, where the electric field has been sampled along the Z direction, 26 mm far away from the probe aperture with and without absorbers. Return loss of the configuration was improved from -20.1 dB to 34.2 dB by adding the absorber. The co-polar and cross-polar far-field pattern of were measured with two probe horns as shown in Figure 10. In Figure 11, the co-polar patterns are compared with an approximate formula for an open-ended waveguide [29] and are consistent with the calculation. The peak of the cross-polar pattern was around -20 dB less than that of the co-polar pattern.
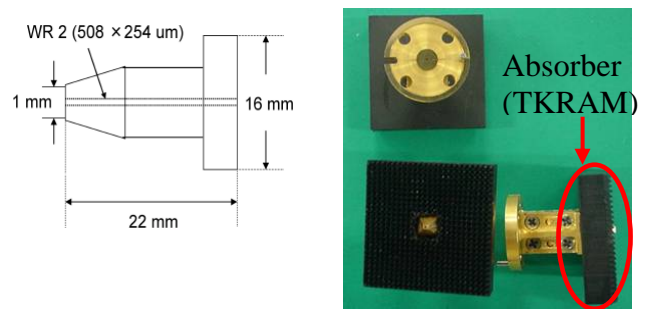

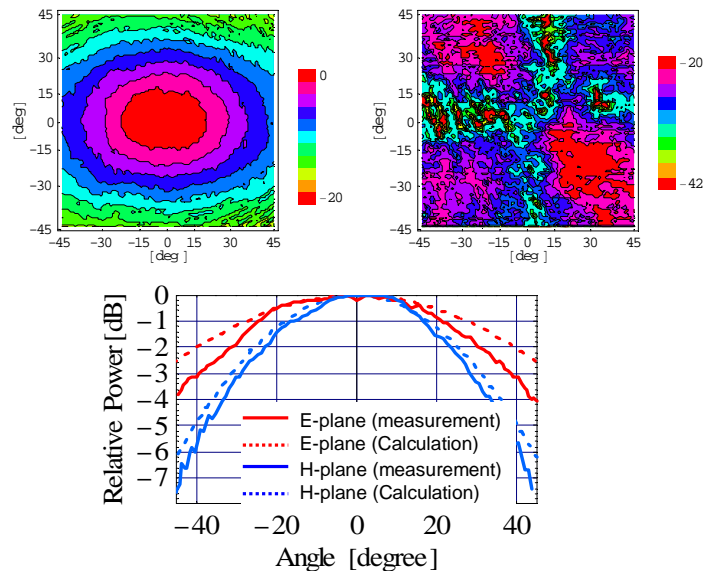Fig. 7 The design (left) and picture (right) of WR2.0 open-ended waveguide horn

Fig. 8 The far-field pattern of WR2.0 open-ended waveguide horn. Co-(upper left) and Cross-polarization (upper right) pattern at 442GHz. The measured far-field pattern compared with the calculation.

IV. RESULTS

The 0.5 mm steps of X and Y stages satisfy the requirement of spatial sampling theorem [30]. Every 5 minutes, phase reference was checked at the center position.

A typical 2-dimensional scan took around 4 hours. Distance between AUT and the probe horn was around 50 mm at the room temperature measurement.

A. Corrugated Horns at Room Temperature

Vector near-field measurements of two corrugated horns at room temperature were taken at 385, 442, 500 GHz. Far-field patterns transformed from near-field measurements of two horns are compared to simulations with CORRUG (Figure 9). The far-field patterns of corrugated horns were found to be identical with each other, very symmetric, low side-lobe, consistent with simulation within a dynamic range of greater than 40 dB, and the peaks of cross-polarization level were -30 dB lower than that of co-polar.

Far-field patterns of the corrugated horn with OMT, which has h-polarization and v-polarization, at 385, 442, and 500 GHz transformed from near-field are shown in Figure 10. The far-field patterns of OMT were also found to be identical with two polarizations, very symmetric and low side-lobe, but the cross-polarization level were slightly higher than corrugated horn only.
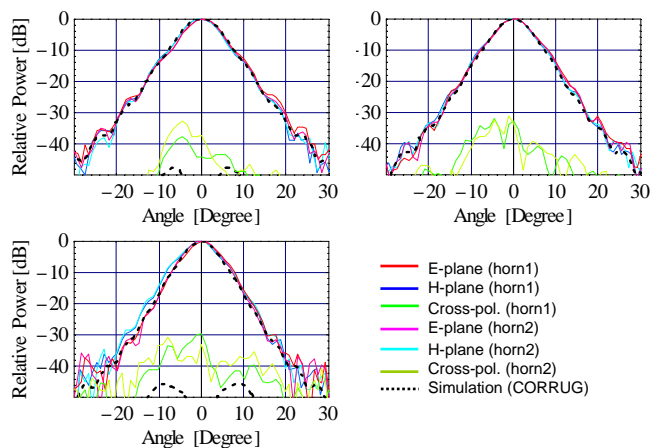

Fig. 9 The far-field pattern of two corrugated horns at 385(upper left), 442(upper right) and 500 GHz(lower).
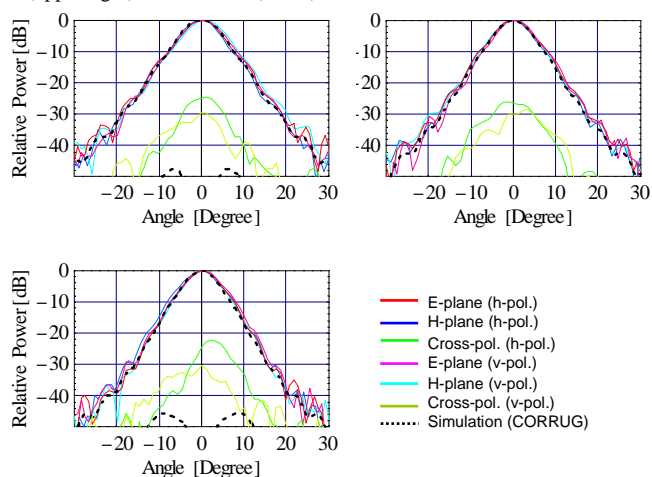

Fig. 10 The far-field pattern of the corrugated horn with OMT at 385(upper left), 442(upper right) and 500 GHz(lower).

B. The Optics block with the Corrugated horn and OMT at Room Temperature

The far-field beam pattern of an optics block of the band 8 cartridge fed by a corrugated horn was measured at room temperature Figure 11, 12. This optics block includes the OMT, an ellipsoidal mirror and the corrugated horn as well as their holding structure. The WR2.0 flange of the corrugated horn was connected to a harmonic mixer and its IF output was fed to the vector voltmeter.

The far-field patterns of optics block were found to be very symmetric, low side-lobe, and consistent with simulation with range from -3.5 to 3.5 degree, with which the beam from mirror of optics block illuminates the sub-reflector of ALMA 12-m. The peaks of Cross-polar were -21.4, -23.3, -20.5 dB lower than that of co-polar at 385, 442, 500 GHz, respectively.
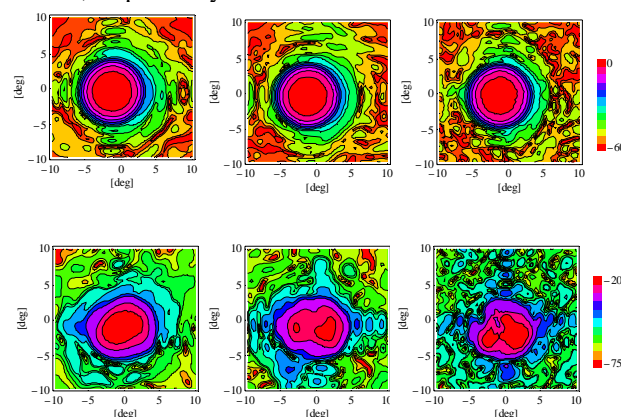

Fig. 11 The far-field pattern of optics block at 385(left), 442(middle) and 500 GHz(right). Upper panels show co-polarization, and lower panels show cross-polarization.
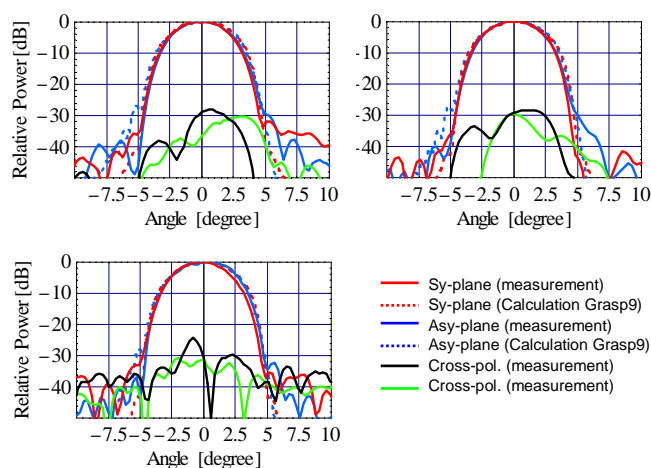

Fig. 11 The far-field pattern of the optics block with the OMT and corrugated horn at 385(upper left), 442(upper right) and 500 GHz(lower).

V. Conclusions

1. We have developed a beam measurement system covering from 385 to 500 GHz, which can measure vector near-fields with wide dynamic range of amplitude (> 50 dB) and stable phase with a high precision XYZθ planar scanner.

2. Beam patterns of corrugated horns for ALMA band 8 cartridge receiver have been measured and compared with simulations at far-field. They are consistent within a dynamic range of greater than 40 dB at three frequencies of 385, 442 and 500 GHz.

3. Beam patterns of the optical block of ALMA band 8 PPM cartridge which includes the ellipsoidal mirrors, the OMT and the corrugated horn have been measured at room temperature and compared with simulations at far-field. They are consistent within a dynamic range 30 dB at the three frequencies of 385, 442 and 500 GHz.

4. The side lobe levels at 385, 442 and 500 GHz of ALMA band 8 receiver were less than −30 dB at far-field. The measured beam patterns correspond to taper efficiency of greater than 92 % at the sub-reflector of the ALMA 12 m antenna.

REFERENCES

[1] Kamikura M. et al. "Development of a 385-500 GHz Orthomode Transducer (OMT).", This conference.

[2] Brown, R. L. et al., "Alma - the atacama large millimeter array." Advances in Space Res. 24, 555 - 559 (2004)

[3] Carter, M. C.et al., "ALMA front-end optics." SPIE, 5489, 1074 - 1084 (2004).

[4] Tham, C. Y., Withington, S.,"Receiver optics design electromagnetic analysis, second report (Bands 3, 6,7 and 9)." Tech. rep., Chambridge University (2003).

[5] Tham, C. Y., Withington, S.,"Receiver optics design electromagnetic analysis, third report (Bands 4, 8and 10)." Tech. rep., Chambridge University (2003).

[6] Johnson, R. C. et al., "Determination of far-field antenna patterns from near-field measurements." Proc. ofthe IEEE, 61, 1668 - 1694 (1973) M. Shell. (2002)

[7] Slater, D."Near-Field Antenna Measurements." Artech House Publishers (1991)

[8] Yaghjian, A. D. "An overview of near-field antenna measurements." IEEE Trans. of Antennas and Propagation, 34 (1986)

[9] Joy, E. B. et al. "Applications of probe-compensated near-field measurements." IEEE Trans. on Antennas and Propagation, 26, 379 - 389 (1978).

[10] Paris, D. T., Leach, W.M.Jr., Joy, E. B. "Basic theory of probe-compensated near-field measurements." IEEE Trans. on Antennas and Propagation, 26, 373 - 379 (1978).

[11] Chen, M.T. et al. "Receiver beam characterization for the SMA." Part of the SPIE Conf. on Advanced Technology MMW, Radio, and THz Telescopes Kona, Hawaii. 106 -113 (1998).

[12] Slater, D. "A 550 GHz near-field antenna measurement system for the NASA submillimeter wave astronomy." Antenna Measurement Techniques Association Conf. (1991).

[13] Tong, C-Y. E. et al. "Near-field characterization of 2-D beam patterns of submillimeter superconducting receivers." Proc. 5th Int. Symp. Space THz Tech., Ann Arbor, MI, 660 - 672 (1994)

[14] Goy, P. et al. "Vector measurements at millimeter and submillimeter wavelength: Fasibility and Applications." Proc. of 2nd ESA Workshop on Millim. Wave Technology and Appl. Antennas, Circuits and Systems, Millilab Espoo, Finland, 89 - 94, (1998)

[15] Tong, C. Y. E. et al."Near field vector beam measurements at 1 THz." IEEE Microwave and Wireless Components Lett. 13, 235 - 237 (2003)

[16] Murk, A., Magun, A. "Characterization of corrugated horn antennas for HIFI." 25th ESA Antenna Workshop on Satellite Antenna Technology, 159 (2002)

[17] Murk, A. et al."Beam pattern measurements of the submillimeter limb-sounder SMILES Ambient Temperature Optics." 3rd ESA Workshop Millim. Wave Technology (2003)

[18] Y. Sekimoto et al. "Development of ALMA Band8 Cartridge and its Measurement System." This conference.

[19] Lamb, J.W. et al. "ALMA receiver optics design." ALMA memo 362(2001)

[20] Murphy, J.A. "Distortion of a single Gaussian beam on reflection from off-axis ellipsoidal mirrors." International J. of Infrared and Millim. Waves 8, 1165-1187 (1987)

[21] Satou, N. et al. "A submillimeter cartridge-type receiver for ALMA Band 8 (385 - 500 GHz) " PASJ in press(2008)

[22] Matsunaga, M. et al. "An experimental study of submillimeter-save horn antennae for a submillimeter-wave astronomy. "PASJ 55, 1051 - 1057 (2003)

[23] Matsunaga, M. et al. "Analysis of submillimeter-wave horn antennas for submillimeter-wave telescopes." Proc. of SPIE, 5445, 446 - 449 (2004)

[24] Naruse M., "Near-field Beam and Cross-polarization Pattern Measurement of ALMA Band 8 Cartridges", to be submitted.

[25] Slater, D. "A 550 GHz near-field antenna measurement system for the NASA submillimeter wave astronomy." Antenna Measurement Techniques Association Conf. (1991)

[26] Slater, D."A large aperture 650 GHz near-field measurement system for the Earth Observing System Microwave Limb Sounder." Antenna Measurement Techniques Association Conf.(2001)

[27] Sekimoto, Y. et al. "Cartridge test cryostats for ALMA front end." ALMA memo 455 (2003)

[28] Richond, J.H.et al. "Probes for microwave near-field measurements." IEEE Trans. on microwave theory and techniques, 3, 32 - 34 (1955)

[29] Yaghjian, A.D. "Approximate formulas for the far field and gain of open-ended rectangular waveguide." IEEE Trans. of Antennas and Propagation, 32, 378 - 384 (1984)

[30] Joy, E.B., Paris, D.T. "Spatial sampling and filtering in near-field measurements." IEEE Trans. on Antennas and Propagation, 20, 253 - 261 (1972)